metals

Article

The Effect of Bi and Zn Additives on Sn-Ag-Cu Lead-Free Solder Alloys for Ag Reduction

Yubin Kang, Jin-Ju Choi, Dae-Guen Kim and Hyun-Woo Shim *

Materials Science & Chemical Engineering Center, Institute for Advanced Engineering, Yongin-si 17180, Korea; ybkang@iae.re.kr (Y.K.); sherapis42@iae.re.kr (J.-J.C.); dgkim@iae.re.kr (D.-G.K.)
* Correspondence: scode@iae.re.kr

Abstract: This study aimed to investigate the effects of the addition of Bi and Zn on the mechanical properties of Sn-Ag-Cu lead-free alloy frequently used as a soldering material in the semiconductor packaging process. To reduce the Ag content of the commercial alloy SAC305 (Sn-3Ag-0.5Cu) by 1 wt.%, Bi and Zn were admixed in different ratios and the changes in mechanical and electrical properties were analyzed. Compared to the SAC305 alloy, electrical conductivity and elongation at break decreased while tensile strength increased following the addition of the two elements. In particular, upon the addition of 1 wt.% Bi, the tensile strength increased to a maximum of 43.7 MPa, whereas the tensile strength was 31.9 MPa in the alloy with 1 wt.% Zn. Differential thermal analysis and scanning electron microscopy revealed that the changes in physical properties can be ascribed to a reduction in the activation energy required for formation intermetallic compound when Bi was added, and the refinement of the structure due to a decrease in undercooling degree when Zn was added. When Bi and Zn were added at the same time, each characteristic for the change in the microstructure was applied in a complex manner, but the effect on the change of the physical properties worked independently.

Keywords: Sn-Ag-Cu alloys; lead-free solder alloys; SAC305; Zn; Bi

Citation: Kang, Y.; Choi, J.-J.; Kim, D.-G.; Shim, H.-W. The Effect of Bi and Zn Additives on Sn-Ag-Cu Lead-Free Solder Alloys for Ag Reduction. *Metals* **2022**, *12*, 1245. https://doi.org/10.3390/met12081245

Academic Editors: Shili Shu and José Spinelli

Received: 7 June 2022
Accepted: 22 July 2022
Published: 25 July 2022

1. Introduction

The Sn-Ag-Cu alloy is a great alternative that can be used for soldering instead of harmful Pb. Sn-Ag-Cu is becoming an essential alloy material for soldering in the electrical and electronic industries owing to its low melting point (~217 °C) and excellent electrical properties [1–5]. As the solder paste used in the semiconductor packaging process contains approximately 90 wt.% soldering metal powder, the physical and mechanical properties of the parent metal, such as tensile strength and electrical conductivity, greatly impact the performance of the soldering equipment. The properties of most commercial Sn-Ag-Cu alloys, such as Sn-4Ag-0.5Cu, Sn-3.8Ag-0.6Cu, Sn-3.7Ag-0.7Cu, Sn-3Ag-0.7Cu, Sn-1Ag-0.5Cu and Sn-3Ag-0.5Cu, are optimized to meet the needs of the final product by precisely controlling the Ag and Cu content [6–10].

Ag is added to the solder alloy owing to its advantageous mechanical fatigue properties and generally accounts for 3–5 wt.% of the alloy, which significantly increase the material cost. Following reports on the physical fragility of joints due to the formation of the coarse Ag_3Sn phase in alloys with a high Ag content, there has been ongoing research to replace it with other alloying elements, such as Mn, Ce, Ni, Ti, Bi, and Zn, to improve the mechanical properties while reducing the material cost [11–13]. In particular, many studies have focused on Zn and Bi as potential substitutes. Kang et al. reported that the undercooling degree can be decreased in the SAC-Zn alloy prepared by adding Zn at 1 wt.% or less to the commercially SAC305 (Sn-3Ag-0.5Cu) alloy, which prevented the formation of coarse Ag_3Sn plate-like phase that adversely affects the plastic deformation properties [14]. Ali et al. reported that adding 1 wt.% Bi to the Sn-Ag-Cu alloy system considerably improved tensile strength as a consequence of grain refinement, but brittleness also increased [15]. However, there is a lack of studies concerning changes in the microstructures and characteristics according to the addition ratio, as well as interference effects when both Zn and Bi are added at the same time.

Herein, we varied the proportion of Bi and Zn added to replace Ag in SAC305 with the total amount of Bi and Zn added fixed at 1 wt.%. Changes in the physical properties and microstructure were investigated.

2. Materials and Methods

The test materials used to conduct the solder alloy casting experiments included Sn, Ag, Cu, Bi, and Zn as the base material (all >99% purity). A 50 kW-class coil-type induction furnace (World Induction Co. Ltd., Incheon, Korea) and a graphite crucible were used for melting. All the equipment and tools used for casting and melting were preheated to 200 °C to remove residual moisture and prevent property changes due to the rapid cooling of the molten metal. The molten Sn alloy of each composition was prepared by gravity casting in a graphite square mold at approximately 500 °C in air atmosphere and the oxide layer was immediately removed in the casting process.

The composition of the prepared samples was analyzed using X-ray florescence (XRF, XRF-1800, SHIMADZU, Kyoto, Japan). Changes in microstructures according to each composition were examined by optical microscopy, field emission scanning electron microscopy (FE-SEM, MIRA-3, TESCAN, Brno, Czech Republic), and energy dispersive X-ray spectroscopy (EDS, Bruker, Billerica, MA, USA). Thermogravimetric/differential thermal analysis (TG/DTA, TG8121, Rigaku, Tokyo, Japan) was used for melting point measurements, as well as pasty range and undercooling degree analyses, while the heating and cooling rates were fixed at a rate of 5 °C/min.

The tensile strength and elongation of the alloy were measured using a universal testing machine (DTU-900MHN, DAEKYUNG, Incheon, Korea) by manufacturing a plate-shaped specimen with dimensions of $25 \times 6 \times 2$ mm^3 (length, width, thickness), meeting the ASTM E8/E8M standard. In this measurement, five samples were prepared for each alloy, and the average value was calculated after measuring five times. Electrical conductivity analysis was conducted using an electrical conductivity meter for non-ferrous metals (SIGMASCOPE SMP350, FISCHER, Waldachtal, Germany). The flat specimens were randomly measured five times to obtain an average value, and the results were converted based on the electrical conductivity of pure copper (58.11 MS/m).

3. Results and Discussion

The aim of this study was to examine changes in the characteristics and microstructures of the SAC305 alloy by substituting 1 wt.% Ag for Bi and/or Zn in various ratios. Table 1 lists the initial elemental compositions of the alloys examined, viz. SAC305, SAC205 + 1 wt.% Bi, SAC205 + 1 wt.% Zn, SAC205 + 0.5 wt.% Bi + 0.5 wt.% Zn, SAC205 + 0.8 wt.% Bi + 0.2 wt.% Zn, and SAC205 + 0.2 wt.% Bi + 0.8 wt.% Zn. Table 2 lists the results of XRF analysis after casting experiments.

Table 1. Elemental compositions before casting Alloys.

Conditions	Elemental Compositions (wt.%)				
	Sn	Ag	Cu	Zn	Bi
SAC305	96.5	3	0.5	-	-
SAC-1Zn	96.5	2	0.5	1	-
SAC-0.8Zn-0.2Bi	96.5	2	0.5	0.8	0.2
SAC-0.5Zn-0.5Bi	96.5	2	0.5	0.5	0.5
SAC-0.2Zn-0.8Bi	96.5	2	0.5	0.2	0.8
SAC-1Bi	96.5	2	0.5	-	1

Table 2. XRF results after casting Alloys.

Conditions	Elemental Compositions (wt.%)				
	Sn	Ag	Cu	Zn	Bi
SAC305	Bal.	3.1358	0.6897	-	-
SAC-1Zn	Bal.	2.1789	0.6273	1.0815	-
SAC-0.8Zn-0.2Bi	Bal.	2.1372	0.5320	0.7897	0.1962
SAC-0.5Zn-0.5Bi	Bal.	2.0045	0.4803	0.3951	0.5028
SAC-0.2Zn-0.8Bi	Bal.	2.0113	0.4716	0.1131	0.7476
SAC-1Bi	Bal.	1.9508	0.6362	0.0662	0.8733

Figure 1 shows the stress-strain curves of the alloys. All six alloys exhibited three stages of deformation: elastic deformation, plastic deformation, and fracture. The SAC305 alloy exhibited strong ductility with a tensile strength of 31 MPa and an elongation of 29.2%. The elongation of SAC-1Zn (26%) slightly decreased compared to that of SAC305, but the tensile strength increased to 31.9 MPa. The tensile strength and the elongation of the alloy containing 0.5 wt.% of Bi and Zn was 38.2 MPa and 21%, respectively. In contrast, when only Bi was added, the ductility (13%) was the lowest, but the tensile strength (43.7 MPa) was the highest. Indeed, the tensile strength of SAC-1Bi increased by ~41% compared to SAC305 while the elongation decreased by ~56%, showing relatively high brittleness, with fracturing occurring immediately after reaching the ultimate tensile strength. Wang et al. reported that the addition of Bi to the Sn alloy increases the brittleness due to the inherent brittleness of Bi element [16].

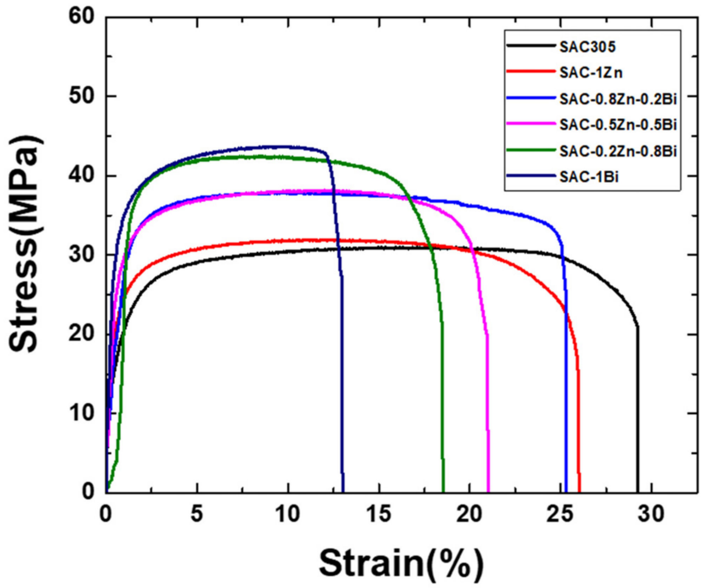

Figure 1. Stress-Strain Curve results according to conditions.

Figure 2 shows the results of electrical conductivity measurements. The SAC305 alloy exhibit an electrical conductivity of 15.28 IACs%. The electrical conductivity of the alloys was approximately 5–10% lower than that of the SAC305 alloy. The electrical conductivity of a metal is a property related to the movement of electrons, which is determined by the complex interplay of factors, such as the purity of constituent elements, average grain size, distribution of grain boundaries, and intermetallic compounds. While the cause cannot be identified based solely on these measurements, in general, the addition of multi-element factors increases the changes in microstructure that adversely affect electrical conductivity, including the formation of intermetallic compounds and changes in activation energy.

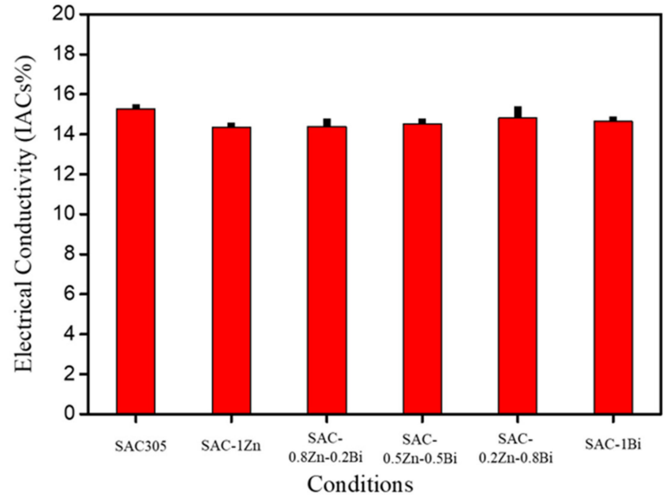

Condition	Electrical Conductivity (IACs%)	
	IACs%	S/m
SAC305	15.28	8.88×10^6
SAC-1Zn	14.36	8.33×10^6
SAC-0.8Zn-0.2Bi	14.38	8.34×10^6
SAC-0.5Zn-0.5Bi	14.52	8.42×10^6
SAC-0.2Zn-0.8Bi	14.82	8.60×10^6
SAC-1Bi	14.64	8.49×10^6

Figure 2. Electrical conductivity measurement results according to conditions.

Figures 3 and 4 and Table 3 show the TG/DTA results of the initial melting point (T_{onset}), the melting end point (T_{end}), the freezing point (T_{cool}), the undercooling degree ($\Delta T_1 = T_{onset} - T_{cool}$), and the solid–liquid coexistence temperature range (i.e., pasty range, $\Delta T_2 = T_{end} - T_{onset}$) of each alloy. For the SAC305 alloy, the undercooling degree and pasty range were measured to be 27.45 and 40.86 °C, respectively. While the undercooling degree was significantly reduced to 6–8 °C for the Zn-containing alloys, the pasty range of the Bi-containing alloys increased by approximately 2–6 °C. According to previous studies, the addition of a small amount of Zn to the Sn-Ag-Cu alloy system causes a decrease in the undercooling degree and it reduces the large Ag_3Sn phase, which can negatively affect the reliability of the solder joint [14,17,18].

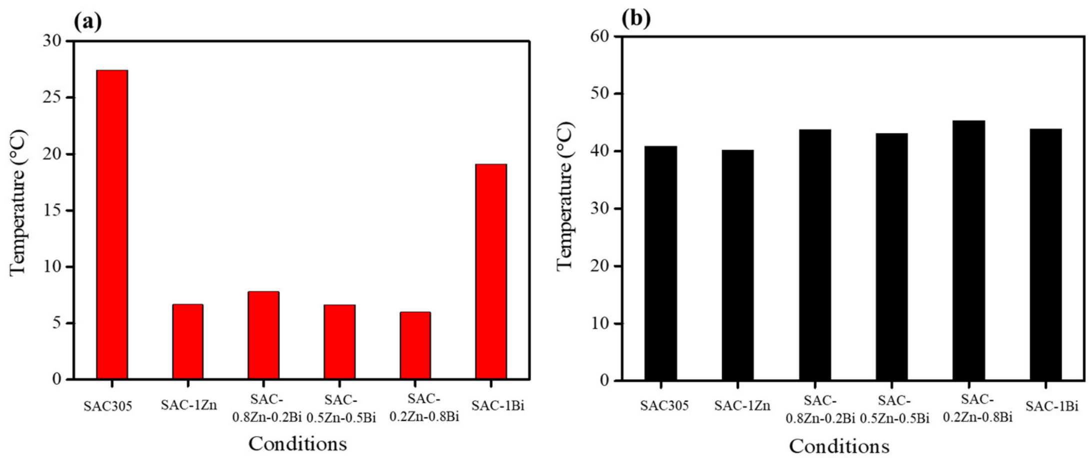

Figure 3. (**a**) Undercooling ($\Delta T_1 = T_{onset} - T_{cool}$) and (**b**) Pasty range ($\Delta T_2 = T_{end} - T_{onset}$) results.

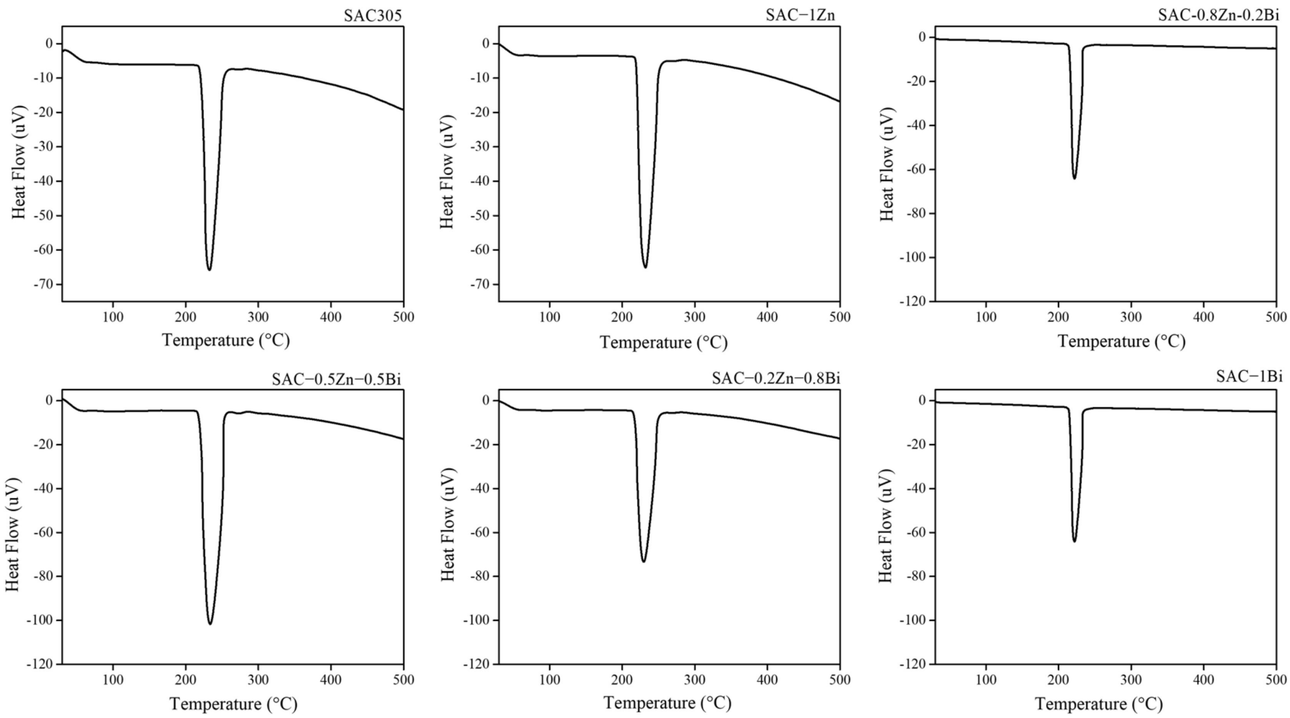

Figure 4. DTA results of experimental alloys.

Table 3. Melting Temperature, undercooling and pasty range of experimental conditions.

Conditions	Onset Melting Point (T_{onset})	End Melting Point (T_{end})	Peak Cooling Point (T_{cool})	Undercooling ($\Delta T_1 = T_{onset} - T_{cool}$)	Pasty Range ($\Delta T_2 = T_{end} - T_{onset}$)
SAC305	217.16 °C	258.16 °C	189.71 °C	27.45 °C	40.86 °C
SAC-1Zn	215.57 °C	255.79 °C	208.91 °C	6.66 °C	40.22 °C
SAC-0.8Zn-0.2Bi	213.61 °C	257.38 °C	205.81 °C	7.80 °C	43.77 °C
SAC-0.5Zn-0.5Bi	214.93 °C	258.02 °C	208.28 °C	6.65 °C	43.09 °C
SAC-0.2Zn-0.8Bi	213.30 °C	258.66 °C	207.32 °C	5.98 °C	45.36 °C
SAC-1Bi	213.33 °C	257.22 °C	194.21 °C	19.12 °C	43.89 °C

Figure 5 shows FE-SEM images and EDS results of the alloys. The addition of Bi is known to cause changes in the microstructure of Sn-Ag-Cu alloys due to an increase in the activation energy to form intermetallic compounds. Zhao et al. reported that the increase in activation energy due to the addition of Bi may interfere with the formation of intermetallic compounds [19]. Similarly, Li et al. reported that the addition of 1 wt.% Bi reduced the nuclear growth rate by increasing the activation energy, thereby inhibiting the growth of intermetallic compounds [20]. Additionally, Illés et al. reported that the addition of Bi in Sn alloy could cause whisker growth [21,22].

On the other hand, upon the addition of Zn to the Sn-Ag-Cu alloy, intermetallic compounds such as γ-$(Cu,Ag)_5Zn_8$ are formed, which acts as Ag acceptors, promoting the growth of the β-Sn phase [17]. Therefore, it is inferred that the γ phase suppresses the formation of the Ag_3Sn phase, thereby reducing the undercooling degree. As evident from Figure 4, the typical Cu_6Sn_5 and Ag_3Sn phases are distributed in the Sn matrix of SAC305. With the addition of 1 wt.% Zn, the γ-$(Cu,Ag)_5Zn_8$ phase is present in a wide area, with the Ag_3Sn phase confined to small regions compared to that of SAC305.

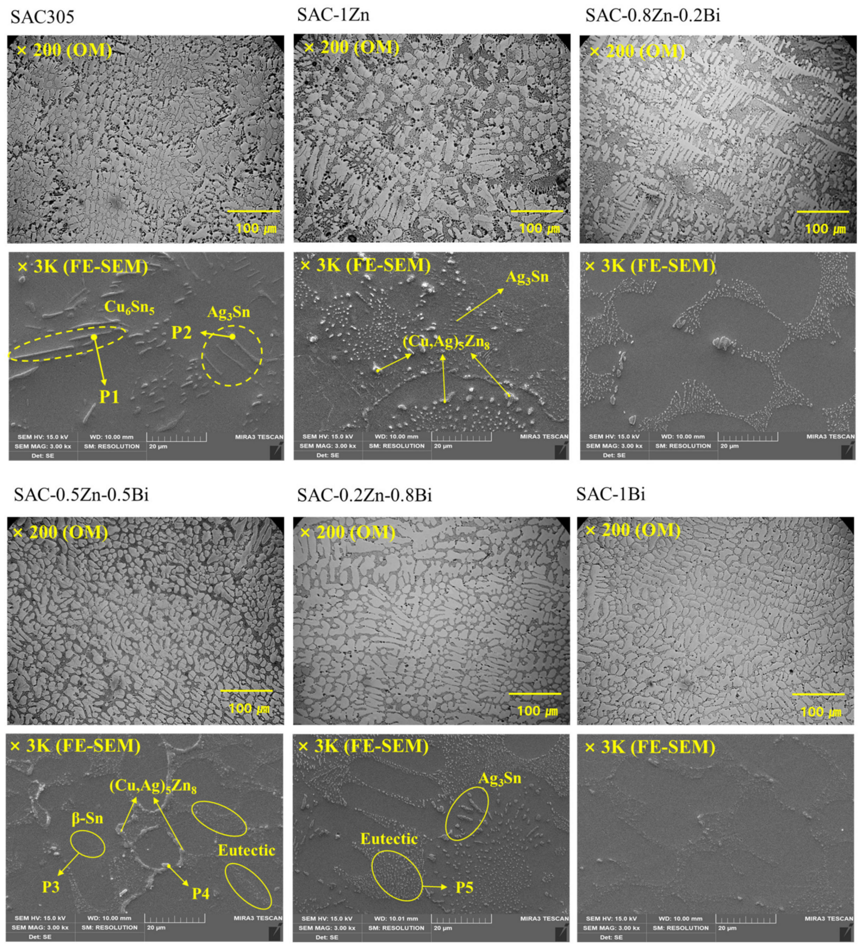

Point	Elements (wt.%)				
	Sn	Ag	Cu	Bi	Zn
P1	52.64	0.18	47.18	-	-
P2	45.87	54.06	0.07	-	-
P3	98.22	-	1.40	0.39	-
P4	5.61	14.27	27.19	-	52.43
P5	82.56	5.22	2.47	9.75	0.20

Figure 5. FE-SEM, OM images and EDS results of each alloy under different magnifications.

The behavior of the Ag_3Sn phase in solder joints has been elucidated through fatigue tests [23,24]. Although it is not clear whether the Ag_3Sn phase promotes or hinders crack propagation, it is known that the Ag_3Sn plate phase can cause localization of plastic deformation at the boundary of the β-Sn phase and adversely affect mechanical properties [14,25]. Therefore, control of the formation of coarse Ag_3Sn phase through the addition of Zn is expected to improve the reliability of the solder joint.

The eutectic fraction decreases upon increasing Bi content, while the size of the intermetallic compound gradually decrease. These changes in the overall microstructure are the main cause of the increase in grain boundaries that interfere with electron transport, which enhance physical properties at the expense of electrical conductivity.

In the alloys containing both Bi and Zn, relatively broad and coarse γ-$(Cu,Ag)_5Zn_8$ phases existed, which becomes more refined with increasing Bi content. Therefore, it was difficult to identify coarse structures other than β-Sn in the Bi-rich condition (in SAC-Bi1 alloy).

As a result, Bi and Zn are added together to replace a certain amount of Ag in the Sn-Ag-Cu alloy, causing changes in the microstructure in a complex manner, but the physical property strengthening characteristics due to the addition of 1 wt.% or less of Bi, the undercooling reduction effect due to the Zn addition, and the coarse Ag_3Sn phase reduction effect are maintained. It was confirmed that these effects could act independently.

4. Conclusions

In this study, we investigated the effects of substituting 1 wt.% of Ag in SAC305 for Zn and Bi on the physical properties of the resultant alloys. The tensile strength increased and the elongation decreased as the amount of Bi added increased, which was ascribed to interference with the formation of intermetallic compounds due to an increase in activation energy. Upon the addition of Zn, the undercooling degree drastically decreased even with a small amount added, and refining of the Ag_3Sn phase and other intermetallic phases was confirmed by changes in the microstructure. Additionally, even with 1 wt.% or less of Bi and Zn added at the same time, the microstructure changes were caused by γ-$(Cu,Ag)_5Zn_8$ by production due to the addition of Zn and tissue refinement due to the addition of Bi, in a complex manner. However, the changes in physical properties caused by this did not interfere with one another, with the effects appearing independently.

Author Contributions: Investigation, writing—original draft preparation, Y.K.; formal analysis, writing, J.-J.C.; review and editing, D.-G.K.; project administration, H.-W.S.; All authors have read and agreed to the published version of the manuscript.

Funding: This work was supported by the Technology Innovation Program (20011176) funded by the Ministry of Trade, Industry & Energy (MOTIE, Korea).

Data Availability Statement: Not applicable.

Conflicts of Interest: All the authors of the papers declare no conflict of interest.

References

1. Rettenmayr, M.; Lambeacht, P.; Kemp, B.; Graff, M. High melting Pb-free solder alloys for die-attach applications. *Adv. Eng. Mater.* **2005**, *7*, 965–969. [CrossRef]
2. Wang, F.J.; Yu, Z.S.; Qi, K. Intermetallic compound formation at Sn–3.0Ag–0.5Cu–1.0Zn lead-free solder alloy/Cu interface during as-soldered and as-aged conditions. *J. Alloys Compd.* **2007**, *438*, 110–115. [CrossRef]
3. Gain, A.K.; Chan, Y.C.; Sharif, A.; Wong, N.B.; Yung, W.K.C. Interfacial microstructure and shear strength of Ag nano particle doped Sn-9Zn solder in ball grid array packages. *Microelectron. Reliab.* **2009**, *7*, 746–753. [CrossRef]
4. Anderson, I.E.; Harring, J.L. Elevated temperature aging of solder joints based on Sn–Ag–Cu: Effects on joint microstructure and shear strength. *J. Electron. Mater.* **2004**, *33*, 1485–1496. [CrossRef]
5. Islam, M.N.; Chan, Y.C.; Sharif, A.; Rizvi, M.J. Effect of 9 wt.% in addition to Sn3.5Ag0.5Cu solder on the interfacial reaction with the Au/NiP metallization on Cu pads. *J. Alloys Compd.* **2005**, *396*, 217–223. [CrossRef]
6. Gu, X.; Chan, Y.C.; Yang, D.; Wu, B.Y. The shearing behavior and microstructure of Sn–4Ag–0.5Cu solder joints on a Ni–P–carbon nanotubes composite coating. *J. Alloys. Compd.* **2009**, *468*, 553–557. [CrossRef]
7. Hodulova, E.; Palcut, M.; Lechovič, E.; Šimeková, B.; Ulrich, K. Kinetics of intermetallic phase formation at the interface of Sn–Ag–Cu–X (X= Bi, In) solders with Cu substrate. *J. Alloys Compd.* **2011**, *509*, 7052–7059. [CrossRef]
8. Yen, Y.W.; Syu, R.S.; Chen, C.M.; Jao, C.C.; Chen, G.D. Interfacial reactions of Sn–58Bi and Sn–0.7Cu lead-free solders with Alloy 42 substrate. *Microelectron. Reliab.* **2014**, *54*, 233–238. [CrossRef]
9. Hu, X.; Li, Y.; Min, Z. Interfacial reaction and IMC growth between Bi-containing Sn0. 7Cu solders and Cu substrate during soldering and aging. *J. Alloys Compd.* **2014**, *582*, 341–347. [CrossRef]
10. Wang, H.; Hu, X.; Jiang, X. Effects of Ni modified MWCNTs on the microstructural evolution and shear strength of Sn-3.0Ag-0.5 Cu composite solder joints. *Mater. Charact.* **2020**, *163*, 110287. [CrossRef]
11. El-Daly, A.A.; El-Hosainy, H.; Elmosalami, T.A.; Desoky, W.M. Microstructural modifications and properties of low-Ag-content Sn–Ag–Cu solder joints induced by Zn alloying. *J. Alloys Compd.* **2015**, *653*, 402–410. [CrossRef]
12. Chen, Y.; Meng, Z.C.; Gao, L.Y.; Liu, Z.Q. Effect of Bi addition on the shear strength and failure mechanism of low-Ag lead-free solder joints. *J. Mater. Sci. Mater. Electron.* **2021**, *32*, 2172–2186. [CrossRef]
13. El-Daly, A.A.; El-Taher, A.M.; Gouda, S. Development of new multicomponent Sn–Ag–Cu–Bi lead-free solders for low-cost commercial electronic assembly. *J. Alloys Compd.* **2015**, *627*, 268–275. [CrossRef]
14. Kang, S.K.; Shih, D.Y.; Leonard, D.; Henderson, D.W.; Gosselin, T.; Cho, S.-I.; Yu, J.; Choi, W.K. Controlling Ag3Sn plate formation in near-ternary-eutectic Sn-Ag-Cu solder by minor Zn alloying. *JOM* **2004**, *56*, 34–38. [CrossRef]
15. Ali, U.; Khan, H.; Aamir, M.; Giasin, K.; Habib, N.; Owais Awan, M. Analysis of microstructure and mechanical properties of bismuth-doped SAC305 lead-free solder alloy at high temperature. *Metals* **2021**, *11*, 1077. [CrossRef]

16. Wang, F.; Chen, H.; Huang, Y.; Liu, L.; Zhang, Z. Recent progress on the development of Sn–Bi based low-temperature Pb-free solders. *J. Mater. Sci. Mater. Electron.* **2019**, *30*, 3222–3243. [CrossRef]
17. Peng, Y.Z.; Li, C.J.; Yang, J.J.; Zhang, J.T.; Peng, J.B.; Zhou, G.J.; Cun, J.P.; Yi, J.H. Effects of Bismuth on the Microstructure, Properties, and Interfacial Reaction Layers of Sn-9Zn-xBi Solders. *Metals* **2021**, *11*, 538. [CrossRef]
18. Luo, Z.B.; Zhao, J.F.; Gao, Y.J.; Wang, L. Revisiting mechanisms to inhibit Ag3Sn plates in Sn–Ag–Cu solders with 1 wt.% Zn addition. *J. Alloys Compd.* **2010**, *500*, 39–45. [CrossRef]
19. Zhao, J.; Qi, L.; Wang, L. Effect of Bi on the kinetics of intermetallics growth in Sn-3Ag-0.5Cu/Cu solder joint. In Proceedings of the Conference on High Density Microsystem Design and Packaging and Component Failure Analysis, HDP'06, Shanghai, China, 27–28 June 2006; IEEE: Piscataway, NJ, USA, 2006; pp. 232–235.
20. Li, G.Y.; Shi, X.Q. Effects of bismuth on growth of intermetallic compounds in Sn-Ag-Cu Pb-free solder joints. *Trans. Nonferrous Met. Soc. China* **2006**, *16*, s739–s743. [CrossRef]
21. Illés, B.; Hurtony, T.; Medgyes, B.; Krammer, O.; Dusek, K.; Busek, D. Sn and Bi whisker growth from SAC0307-Mn07 and SAC0307-Bi1-Mn07 ultra-thin film layers. *Vacuum* **2021**, *187*, 110121. [CrossRef]
22. Illés, B.; Bátorfi, R.; Hurtony, T.; Krammer, O.; Harsányi, G.; Pietrikova, A.; Skwarek, A.; Witek, K. Whisker Development from SAC0307-Mn07 Solder Alloy. In Proceedings of the 43rd Internation Spring Seminar on Electronics Technology (ISSE), Demanovska Valley, Slovakia, 14–15 May 2020; IEEE: Piscataway, NJ, USA, 2020; pp. 1–5.
23. Kang, S.K.; Lauro, P.; Shih, D.Y.; Henderson, D.W.; Bartelo, J.; Gosselin, T.; Steave, R.C.; Charles., G.; Karl., P.; Choi, W.K. The microstructure, thermal fatigue, and failure analysis of near-ternary eutectic Sn-Ag-Cu solder joints. *Mater. Trans.* **2004**, *45*, 695–702. [CrossRef]
24. Terashima, S.; Kariya, Y.; Hosoi, T.; Tanaka, M. Effect of silver content on thermal fatigue life of Sn-xAg-0.5Cu flip-chip interconnects. *J. Electron. Mater.* **2003**, *32*, 1527–1533. [CrossRef]
25. Kim, K.S.; Huh, S.H.; Suganuma, K. Effects of cooling speed on microstructure and tensile properties of Sn–Ag–Cu alloys. *Mater. Sci. Eng. A* **2002**, *333*, 106–114. [CrossRef]